

# Exploiting the scanning sequence for automatic registration of large sets of range maps

Paolo Pingi<sup>1</sup>, Andrea Fasano<sup>2</sup>, Paolo Cignoni<sup>2</sup>, Claudio Montani<sup>2</sup>, Roberto Scopigno<sup>2</sup>

<sup>1</sup>INOA - Istituto Nazionale di Ottica Applicata, Firenze, Italy

<sup>2</sup>Visual Computing Lab, ISTI-CNR, Pisa, Italy

---

## Abstract

*Range map registration is still the most time consuming phase in the processing of 3D scanning data. This is because real scanning sets are composed of hundreds of range maps and their registration is still partially manual. We propose a new method to manage complex scan sets acquired by following a regular scanner pose pattern. Our goal is to define an initial adjacency graph by coarsely aligning couples of range maps that we know are partially overlapping thanks to the adopted scanning strategy. For a pair of partially overlapping range maps, our iterative solution locates pairs of correspondent vertices through the computation of a regular  $n \times n$  kernel which takes into account vertex normals and is defined in the 2D space of the range map (represented in implicit 2D format rather than as a triangle mesh in 3D space). The shape-characterization kernel and the metrics defined give a sufficiently accurate shape matching, which has been proven to fit well the requirements of automatic registration. This initial set of adjacency arcs can then be augmented by the automatic identification of the other significant arcs, by adopting a criterion based on approximate range map overlap computation. With respect to the solutions present in literature, the simplifications and assumptions adopted make our solution specifically oriented to complex 3D scanning campaigns (hundreds of range maps). The proposed method can coarsely register range maps in parallel with the acquisition activity and this is a valuable help in assessing on site the completeness of the sampling of large objects.*

Categories and Subject Descriptors (according to ACM CCS): I.4.8 [Scene Analysis]: Range data

*Keywords:* 3D scanning, automatic registration, coarse registration, range map alignment.

---

## 1. Introduction

The increasing use of 3D scanning devices and the design of new and efficient algorithms for range data post-processing are the basis of a process where standard CAD tools are going to be replaced by a semi-automatic process based on the direct sampling of real objects' shape. Moreover, automatic acquisition of shape and appearance is no longer confined to the classical industrial applications (reverse engineering or quality control), but it is positively affecting new and important fields, such as Cultural Heritage (CH). Unfortunately, the creation of 3D digital models from reality is still far from being as simple as photography. The user has to manage many complex processing steps (range maps acquisition, registration, fusion, geometry simplification, color attribute recovery). A current goal is to design new solutions which transform the scanning pipeline into an unattended process.

In this direction, at present, it is possible to assert that the bottleneck of the whole process is the *range maps registration* phase, since this is the only task where a considerable human intervention is still required. The accurate acquisition of a real object requires many range maps taken from different locations. If the scanner location and orientation are not tracked, all those range maps are produced in different coordinate spaces (each one depending on the corresponding unknown location and orientation of the scanner). The goal of the range map registration phase is to determine the rigid geometric transformations necessary to bring back all the coordinates of the acquired data into a unique Cartesian space. Registration is the fundamental precondition to merge all the data into a single and complete digital model. Our goal is to design new solutions to make the alignment of range maps an automatic process.

The registration of multiple scans is usually implemented by adopting a software approach split into two computational steps. An initial *coarse registration* provides a rough positioning of the range maps, and a subsequent *fine registration* brings the scans into tight alignment. In other words, coarse registration is concerned primarily with determining which regions of two scans represent the same portion of the object's surface if any (the so called pair-wise surface matching, to align them on the "overlapping" region), while fine registration is concerned with minimizing the mismatch between these corresponding overlapping regions. *Fine local* pair-wise registration [BM92, LR01] or *fine global* registration (extended to the whole scanning set [Pul99]) are generally based on unattended iteration of the ICP technique and by now they ensure extremely good performances and results. On the other hand, *coarse* registration represents the real bottleneck. Despite the number of solutions proposed (see Section 2), most of the available software systems implement the coarse registration adopting a time-consuming, interactive approach. According to the experience of the authors, a complex scanning set composed of some hundreds of range maps can require several days of difficult and tedious work to process the manual coarse registration phase.

This paper presents an efficient automatic solution to the problem of the range maps registration. Even though many algorithms and techniques exist in literature that provide excellent and general solutions (see Section 2), the objective of the current work is to manage efficiently a very large amount of data resulting from real scan campaigns. In order to achieve this goal, our method is based on two assumptions:

1. the initial adjacency relations between the range images are implicitly derived from the scanning pattern used during the acquisition phase;
2. during the acquisition the scanner device does not rotate "significantly" along its view direction (a plausible assumption, since it's usually placed over a tripod).

In this paper we present a different approach to the multi-view registration task based on the idea that during a real scan campaign the acquisition phase is usually performed following some sort of regular pattern: horizontal, vertical or circular. The pattern used to acquire range maps implicitly defines an initial adjacency graph that can be used to start the process by computing pair-wise range maps matching for the coarse registration. The new metric proposed for pair-wise matching is fast to compute and easy to implement. Then, the system is able to augment the adjacency graph by introducing all other registration arcs corresponding to pair of range maps with significant overlap extent.

The advantages of our solution are as follows:

- *Simplicity and generality*: the method does not require HW tracking systems and can be applied to any scale (from small objects to buildings).

- *Exploiting available knowledge*: scanning CH artifact is moving from a research issue to a "standard" activity that just like any other documenting task should necessarily include some kind of planning, producing a regular scanning scheme to be faithfully followed during the 3D scanning process. Random scanning is not quite common in the case of complex scanning activities. 3D scanning is becoming a structured process and it is unreasonable that a complex activity involving the documentation of large valuable CH objects proceeds without any kind of order. Scanning is therefore a planned, structured task and exploiting this information should not be seen as an hack or a trick but as an opportunity to avoid wasting valuable information. As we will see in the following, we make proficient use of the information on the acquisition pattern.
- *Scalability*: existing approaches have been tested only on very small datasets that are 1 or 2 mag orders less than the real-world complex scans (i.e. 1-5 million points vs. hundred million points). Scalability of other multi-view surface matching is limited to small scan sets (less than 50 range maps, according to [HH03]). Our method has been proved to work on a very complex scanning set (up to 300 range maps).
- *Robustness*: existing global approaches can fail in the case of *symmetries* along part of the objects. Focusing on small portions of the objects (the ones covered by the overlapping sections of high-resolution range maps, which usually cover a very small subset of the object) increases the probability of finding erroneous self-similarities. This is even more critical when scanning artworks, since the presence of symmetry is not a pathological situation but the common use case: decoration is often a matter of repeating symmetric patterns (see Figure 6). The probability of producing wrong matches grows quadratically with the size of the dataset (the number of possible range maps pairs grows quadratically), and detecting and purging them is not easy. On the other hand, a linear approach such as the one proposed here reduces the possibilities of producing wrong matches.
- *Accuracy*: other approaches use a graph-based approach [HH03, BDW\*04], where a *minimum spanning tree* of the graph of all possible pair-wise registration is built and defines the global registration. On the other hand, our global alignment is built on a subset of the graph (a connected sub-graph possibly cyclic, not a tree), defined by adopting a criterion based on the percentage of spatial overlap between range maps (see Section 5). This means that much more data is used in the registration and the overall quality of results is improved. The final registration accuracy in all our tests is well below a maximal error of 0.1 mm.
- *Usability*: previous approaches adopt a *do-everything* or *fail* approach. From an engineered point of view, our approach never totally fails. As we will see in the following, even if a single pair-wise surface matching fails (a very rare occurrence in our tests) the work done on all other matches can be used proficiently by simply adding a

single manual alignment to the previous coarsely aligned maps. This manual intervention can also be used for the rough alignment of the range maps eventually acquired beyond the regular pattern.

To our knowledge, our solution is the only one experimented with success on really complex scanning campaigns (i.e. hundreds of range maps representing objects which do not fit the working volume of the scanning device).

## 2. Related work

The alignment task is the most time-consuming phase of the entire 3D scanning pipeline, due to the substantial user contribution required by current systems, since range map registration is usually solved by adopting a partially manual process. The standard approach is as follows:

### Local pairwise registration

- *Overlapping range maps detection*: for each range map  $R_i$  in the scan set  $\bar{R}$ , detect all  $R_j$  in  $\bar{R}$  which are partially overlapping with  $R_i$ . This pairwise process can be considered as a graph problem: given the nodes (i.e. the range maps), we have to select a subset of arcs such that every node is linked to some others if the corresponding maps are partially overlapping, and thus have to be aligned (*graph of overlaps*). If the set of range maps is composed of hundreds of elements (the scanning of a 2 meters tall statue generally requires between 200 and to 500 range maps, depending on the device used and on the shape complexity of the object), then the user has a very complex task to perform;
- *Initial coarse registration*: provide a first rough registration for each range map. This is performed by deriving from the complete graph of overlaps a subgraph in which (a) each node (range map) has at least one entering arc, (b) the graph is connected, i.e., for every couple of nodes  $i$  and  $j$ , a path connecting  $i$  and  $j$  exists. The initial placement is heavily user-assisted in most of the commercial and academic systems. It usually requires the interactive selection and manipulation of the range maps, either to select a small set of corresponding point pairs or to superimpose the range maps by means of interactive rotations and/or translations;
- *Fine Pairwise Registration*: the scans are finely aligned, usually adopting the Iterative Closest Point process (ICP) [BM92, CM92, LR01] which minimizes the alignment error between any pair of range maps.

### Global registration

- The pairwise registration produces good results but, since the error minimization takes place sequentially on mesh pairs, the error tends to accumulate and it may result in significant artifacts after a number of pairwise steps. A solution is to perform a global minimization process which distributes the residual error among all pairs in order to spread the error evenly among all range map pairs [Pul99].

The precision of the *coarse registration* phase does not need to be really high because the convergence of the successive *fine registration* is ensured even when the accuracy is low (e.g. a few millimeters of distance between the two maps); however, the manual intervention required for coarse registration is time-consuming and boring, since it usually requires several days of work on a complex scanning set.

## 2.1. Hardware tracking

An orthogonal strategy to the one presented here is to add a tracking subsystem to the scanning device to track its position and orientation in the scanning space. *Tracking solutions* can be based on multiple technologies: magnetic trackers [Pol03], optical trackers [Ste04], or accurate mechanical systems (like rotary platforms or robotic arms [LPC\*00, CFI\*04]) which can produce all needed data on the translation/rotation of the object/scanner.

## 2.2. Pair-wise matching and automatic registration

*Automatic coarse registration* was investigated quite intensively in the last years; it is possible to distinguish different approaches to solve the problem. It's not our intention to present here a complete survey of the algorithms proposed in the literature (a good overview can be found in [CF01, HH03]).

Roughly speaking the methods for pair-wise matching of range maps can be subdivided into at least three large classes: methods based (a) on the rigidity of the shape, (b) on the global characterization of the shape, and (c) on the local characterization of the shape.

In the methods based on the *rigidity of the shape* the 3D registration problem is treated as a partial matching problem and the rigidity constraint among some preselected control points is exploited to restrict the search range used for matching. A representative of this class is the well-known DARCES [CHC99] algorithm, an approach based on the RANSAC scheme [FB81], that is invariant for all kind of rotations and translations. The methods of this class are generally robust, they get a solution also in presence of noise of the data, and they do not need that the data contain local features. On the other hand these methods are computationally intense.

The methods based on the *global characterization of the shape* generally define a mapping from the surface model to some fixed-dimensional vector space. Delingette et al. ([DHI92, DHI93]) developed the *Spherical Attribute Image* (SAI) method that defines a direct mapping between an object surface and a spherical surface, thus obtaining a unique representation of any non-convex object (or part of it); the correspondence between two range maps can be obtained from a comparison of the respective SAIs. A similar approach is represented by the *spherical extent function* [VS01]. Harmonic maps have been adopted

as surface descriptors, among others, by Funkhouser et al. [MKR03]. They proposed the *spherical harmonic representation* which provides a rotationally invariant representation of a shape descriptor based on spherical harmonics, enhanced in [MKR04] by factoring out the contribution of anisotropy and geometry. Lucchese et al. [LLC02] introduced a method operating in the *frequency domain*: to estimate the roto-translation between a pair of meshes they propose a featureless algorithm which exploits the information about the geometric regularity captured by the Fourier transform. These methods generally suffer for noise in the data, insufficient overlap between the surfaces and high computational costs.

The methods based on the *local characterization of the shape* are generally more appropriate than the previous ones because they do not suffer in the cases of highly incomplete knowledge of the surfaces to be aligned. The *object-based* approach of the previous class is replaced by a *vertex-based* approach. Most of the methods use some sort of evaluation of the curvature of the mesh to characterize mesh vertices (bi-tangent curves are used, for example, in [WG02]). Stein and Medioni [SM92] introduced the *splash images*, i.e. small surface patches used to detect local changes in the surface orientation. *Splash images* are then used as primitives to measure the differences between surface normal distributions (this proposal was one of the main inspirations for our work). Chua and Jarvis [CJ97] proposed the *point signature*, a representation invariant to rotation and translation that encodes the minimum distances of the points on a 3D contour (intersection of the surface with a sphere centered in the point under analysis) to a reference plane. *3D point fingerprints* [SPK\*03] can be considered an extension of the previous approach. The point fingerprint is a set of 2-D contours that are the projections of geodesic circles onto the tangent plane. Johnson and Hebert [JH97] proposed the concept of *spin image*, a more descriptive structure than *splash images* and *point signatures*. A *spin image* is generated using oriented points (3D points with directions) and it is a 2D histogram of the surface locations around a point. Matching points that rely on different views of the model have similar *spin images*, so they can be used to find the correct correspondences. Spin images have been recently extended to include texture information which could be encoded in range maps [BAGC05]. Another interesting approach is the one proposed recently by Bendels et al. [BDW\*04], where 2D intensity images are exploited for finding corresponding points on 3D views.

These methods can be used for the coarse registration problem and they generally present good rates of convergence. The main problem is that the generality of the solution is paid in terms of high computational costs.

The availability of color or other surface attributes sampled together with the geometry has been used either to improve the accuracy of geometric registration or to perform automatic coarse alignment [Rot99].

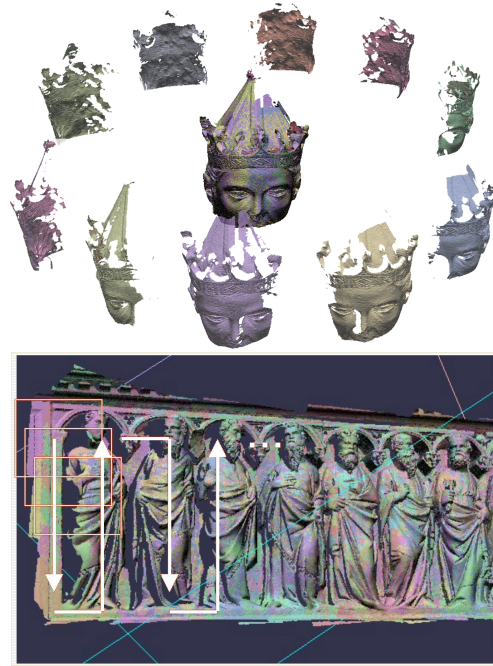


**Figure 1:** Range maps are taken in a row-wise order: an example of circular stripe (top) around a statue's head; an example of raster-scan scanning order (bottom) adopted for the acquisition of a bas-relief.

### 3. Using the information on the scanning plan

The standard registration task of multiple range maps can be simplified by considering some practical aspects. First, since 3D acquisition is usually carried on by following a simple selection of the scanner poses, an initial set of pair-wise matches can be retrieved easily. Users usually acquire range maps in *stripes*, following either a *vertical*, *horizontal*, *raster-scan* or *circular* placement of the scanning system (see Figure 1). The different types of stripes share some common properties: they contain an ordered set of  $n$  range maps, such that range map  $R_i$  holds a significant overlapping with at least  $R_{i-1}$  and  $R_{i+1}$ . Vertical, horizontal or raster-scan stripes are often produced when acquiring objects like bas-reliefs, walls or planar-like items. Circular stripes are indeed more useful when acquiring objects like statues, columns or cylindrical-shaped objects.

If we can assume that the acquisition has been performed using one of these stripe-based patterns, then we may restrict the search for pair-wise matching to each pair of consecutive range maps  $(R_i, R_{i+1})$ . From the point of view of the registration algorithm, all the stripe patterns defined above are equivalent: an automatic registration module can process each couple  $(R_i, R_{i+1})$  to generate the roto-translation transformation matrix  $M_i$  that aligns  $R_{i+1}$  to  $R_i$ . Therefore, we reduce a 1 over  $n$  problem into a 1 over 1 problem. The

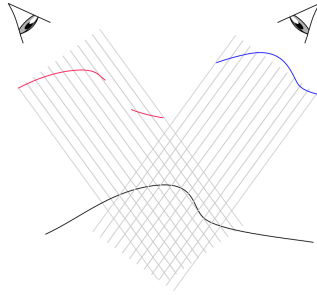


**Figure 2:** Example of silhouette edges or self occlusion between two successive view points.

subset of registration arcs defined above is usually sufficient for a successive ICP application on the selected pairs, in order to obtain a *local* registration. This *stripes-oriented* approach can be seen as an efficient working strategy on complex scanning sets, which maintains computations linear to the number of scans.

#### 4. Automatic pair-wise range map alignment

We assume that the two consecutive range maps  $R_a$ ,  $R_b$ , overlap on a reasonable portion of their surface (15-20%). Like other surface matching algorithms, we look for a small set of *feature points* which characterize the first range map  $R_a$ : a point-based shape description kernel is proposed in Section 4.1. Then, in a second step, for each of these  $t$  points on  $R_a$  we search for the potential corresponding points on the second mesh  $R_b$  (Sec. 4.2). Finally, out of those possible  $t$  pairs, we choose the three matching points giving the best coarse alignment (Sec. 4.3); if the needed accuracy is not reached, we iterate until we get convergence (Sec. 4.4).

##### 4.1. Selection of the starting points

A trivial approach would be to choose the starting points  $p \in R_a$  in a random way over the range map. Unfortunately, this approach can produce non-representative samples that reside in surface areas having little (or no) geometric features and make accurate identification of the corresponding points in the second range map  $R_b$  very hard. For this reason, we need a *measure* of the representativeness of a given vertex for the corresponding range map. Our input meshes are regularly sampled *2D height fields*<sup>†</sup>. The height field assumption gives us a simple local parameterization of the surface that allows, for each point  $p$ , to easily detect a small and regular kernel of adjacent samples and to compute the

<sup>†</sup> This assumption does not hold for some rather unusual situations (like for example the use of a scanner based on an irregular sampling pattern)

variance of  $p$  with respect to the samples. Given a *pivot* vertex  $p \in R_a$  and its normal vector  $N_p$ , we build a *kernel*  $K_p$  by considering the  $n \times n$  points around  $p$  in the range map (represented as a 2D raster). In our implementation, we adopt a  $13 \times 13$  kernel. Each element  $k_{i,j} \in K_p$  contains the dot product of the pivot's normal vector and the normal vector of the corresponding pivot's neighbor. Then, we calculate the variance of each kernel  $K_p \in R_a$ :

$$s^2(K_p) = \frac{1}{n^2} \sum_{i,j} (k_{i,j}^p - \mathbf{E}[K_p])^2 \quad (1)$$

where  $\mathbf{E}$  is the average of each kernel:

$$\mathbf{E}[K_p] = \sum_{i,j} \frac{k_{i,j}^p}{n^2} \quad (2)$$

The variance is used to cluster all the range map points into buckets characterized by a similar surface curvature. Low values of  $s^2(K_p)$  correspond to flat areas where the normal vectors are relatively uniform. On the contrary, high values of  $s^2(K_p)$  correspond to zones having high curvature. We have chosen to discard all points having either high or low variance, using two opportune threshold values selected according to empirical experience. There are several motivations for this choice. First, we obviously discard *flat areas* because they cannot give sufficient information to detect the corresponding point in the other mesh. We discard also points with *high variance*, even if this could seem less intuitive. First, a high variance vertex could belong to an open boundary (and thus to an incomplete local sampling of the surface); it has to be discarded since the matching range map might have a more complete sampling of the same zone that is unlikely to match the previous one. Second, a high variance vertex could be generated in the proximity of a silhouette vertex (where we have a false step due to a self occlusion of the mesh). These portions of the mesh are misleading because these steps do not exist in reality, but they depend on the scanner location at the time of the acquisition of the range map  $R_a$ ; the same portion of the surface, seen from a different point of view, may have a very different shape descriptor. Figure 2 shows how silhouette edges or self occlusion can create a false high-variance ridge not existing on the surface object.

Once the low- and high-variance vertices have been discarded, a small set of candidate starting points are chosen randomly among the remaining points (the ones with medium variance, see Figure 3).

##### 4.2. Finding a matching point

Given a selected vertex  $p \in R_a$ , we have to find the best matching vertex  $q \in R_b$  (if it exists). The accuracy of the matching algorithm is tightly bound to the metric used for the comparison.

Our method builds on the kernel defined in the previous

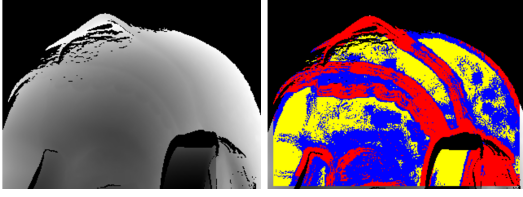


**Figure 3:** Points with medium-variance are shown in blue, high variance in red and low variance in yellow.

subsection: we compute  $K_q$  for every vertex  $q \in R_b$ . Given  $p \in R_a$  and its kernel  $K_p$ , the metric consists of finding the most similar kernel  $K_q$ . For each  $K_q$ , we compute the squared difference with  $K_p$ :

$$d^2(K_p) = \frac{1}{n^2} \sum_{i,j} (k_{i,j}^p - k_{i,j}^q)^2 \quad \forall q \in R_b \quad (3)$$

and we choose as best potential matching point the one having minimum distance  $d^2(K_p)$ .

This metric is invariant with respect to the usual transformations (translations and rotations) occurring to the meshes belonging to a strip. This metric is not invariant to consistent rotations around the view direction of the scanning device. However, in standard 3D scanning activity the scanner is usually placed on a tripod, which makes it impossible to apply a substantial rotation along the view axis.

Obviously, the metric we adopted does not ensure the convergence to the correct matching: the selected corresponding point could be incorrect, since multiple vertices can present a shape signature similar to the one of the vertex considered. Therefore, we need to validate the matching.

Other approaches exist that try to avoid as much as possible any false match by defining more complex shape signatures. We have chosen to follow a strategy which couples a computationally efficient shape descriptor with a further validation phase which proves the correctness of (or purges) the selected matching points pairs.

### 4.3. Matching points validation

By using the approach described in the previous section we get a set  $S$  of  $t$  corresponding points pairs  $(p, q)$  with  $p \in R_a, q \in R_b$  that can include some (or eventually many) false matches. The naive approach – use all the  $t$  pairs to determine the matching transformation matrix  $M$  according to [BM92] – can easily fail if there are many incorrect matching pairs.

The RANSAC (RANdom SAMple Consensus) scheme [FB81] could be used. In the RANSAC algorithm a combination  $Q_j$  of three different pairs in  $S$  should be selected in a random way and then the process iterated until a given threshold is met. We adopted a different approach: since  $t$  is usually small ( $t \leq 30$ ), it is possible to perform an exhaustive search over the  $t$  pairs in order to compute the best roto-

translation matrix. For each combination  $Q_j$  of three different pairs in  $S$  we compute a transformation matrix  $M_j$ . In this way we obtain  $\binom{t}{3}$  different matching matrices  $M_j$ . Then, we choose the matrix that provides the smallest alignment error  $\epsilon_j$  computed only on the 3 pairs in  $Q_j$ :

$$\epsilon_j = \frac{1}{3} \sum_{(p,q) \in Q_j} (\|p - M_j q\|^2) \quad (4)$$

If the alignment error  $\epsilon_j$  is equal or smaller than the user-selected threshold value  $coarse\_err$ , we have found a sufficiently correct alignment. Otherwise,  $M_j$  should not be considered as a correct alignment matrix. This threshold  $coarse\_err$  is usually given in metric units, i.e. in millimeters in our cases.

The computational cost of our approach depends on the value of  $t$  and the resolution of the range maps. Larger is the value of  $t$  and larger is the subset of  $Q_j$  to be considered and checked. In the next paragraph, we will show how to find an alignment matrix using, at each step, a very small value for  $t$  (20 to 40 vertices, where a standard range map contains around 300K vertices).

### 4.4. Iterative matrix computation

If the best transformation matrix found yields an error greater than the given threshold  $\epsilon_{best} > coarse\_err$  then the set of  $t$  pairs contains mostly incorrect matches.

Instead of setting a bigger value for the  $t$  parameter, we adopt an iterative approach: all the previous steps (choice of a new set of  $t$  vertex pairs, evaluation of alignment error) are iterated until a proper alignment matrix is found. To improve accuracy and speed up convergence, we reuse in each iteration the best results obtained in the previous cycle.

At iteration  $i$ , we select the local set of  $t$  matching vertices by computing the respective kernels. Then, to find the best roto-translation matrix, we add to the local  $t$  pairs the 3 pairs that generated the best solution found in the previous iteration. In this manner, the space of possible solutions is augmented and this helps the algorithm to converge faster to a consistent solution.

The main drawback of this method is that we might be trapped in a *local minimum*, i.e. when the algorithm is not capable of finding a better solution than the previous one. We detect a local minimum stall by checking if in subsequent iterations the alignment error  $\epsilon_{best}$  doesn't improve. To remove the stall, we perform a perturbation of the best current solution by discarding one of the 3 couples that generated the current solution. According to the results of our empirical experiments (see Section 6), this simple heuristic detected and recovered all local minima stalls. Moreover, in order to detect the occurrence of an impossible match (e.g. when the overlap  $R_a \cap R_b \approx \emptyset$ ), we set a threshold value  $max\_iter$  at the maximum number of iterations allowed.

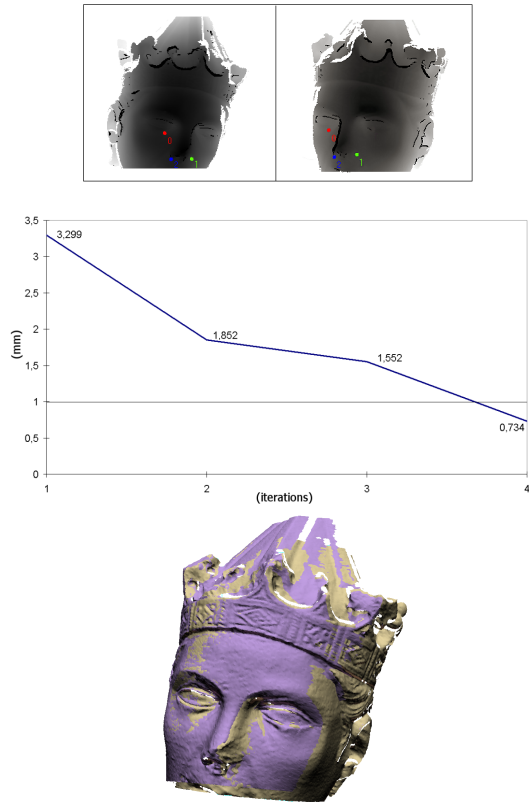


**Figure 4:** The three matching point pairs selected by the algorithm on two range maps (top). The coarse alignment for the two range maps required four iterations (errors are reported in millimeters, middle; this error is further reduced by ICP in the fine registration phase). The result of the coarse alignment of the range maps of the head (bottom).

### 5. Augmenting the adjacency graph

Following the *stripe-based* approach we got a fine local alignment between each subsequent pair of range maps, which is a small subset of all adjacency arcs. Depending on the shape of the object, some more arcs are usually needed to obtain a high-quality alignment (possibly, interconnecting each  $R_i$  with all the overlapping range maps). We do not require a user-assisted, explicit creation of all these arcs. To retrieve all these arcs in unattended mode, augmenting the arcs in our graph of pair-wise alignment, we use a spatial indexing technique. A *discrete space bucketing* data structure can be easily instantiated (3D voxels of size proportional to 5-10 times the inter-sampling distance used in scanning), holding for each bucket the set of range maps passing through that region of space. The initialization of this data structure requires the scan-conversion of every range map in the discrete space. We can easily retrieve groups of overlapping range maps by a simple visit of the bucketing structure, and tell how significant is the overlap extent of each poten-

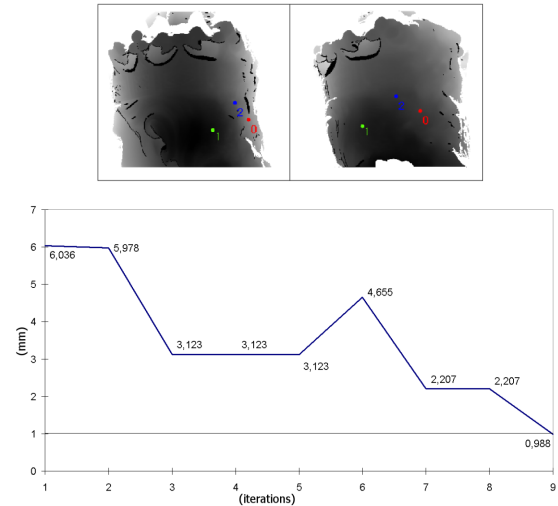


**Figure 5:** The matching point pairs selected on the back of the Arrigo's head; the graph shows the alignment iterations and the two local minima successfully managed.

tial pair by counting the number of buckets which contain the same pair. Obviously, since we reconstruct the discrete occupancy grid at low resolution, the information contained gives an approximation of the overlapping factor and thus a subset of the adjacency graph, but still sufficiently accurate for our purposes. Given the occupancy grid information and once a single alignment arc is provided for each range map (see previous phase), our registration library is able to introduce all needed arcs in a completely unattended manner, by selecting only those which satisfy a minimum-overlap factor, and to process them using the ICP algorithm. Our tool, *MeshAlign* [CCG\*03], implements this type of solution to provide automatic graph completion and local pair-wise and global fine alignment (based on ICP, following [Pul99]). Following our approach, the number of arcs used in the alignment is bigger than the one set up by methods which select a minimum spanning tree over the adjacency graph. In the latter case, we use a number of pair-wise arcs which is equal to the number of range maps minus one. In our case, the larger number of arcs considered in the alignment (see results presented in Table 1) obtains a more accurate overall alignment. Small misalignments are frequent in the case of repeating patterns typical of decorations. In this case, having the same range map involved in multiple alignments allows a more robust and accurate management.

### 6. Experimental results

The proposed registration algorithm was tested on many large datasets coming from real scanning campaigns (each range map is usually affected by noise, artifacts and holes). The laser scanner used in all our acquisitions is a Minolta

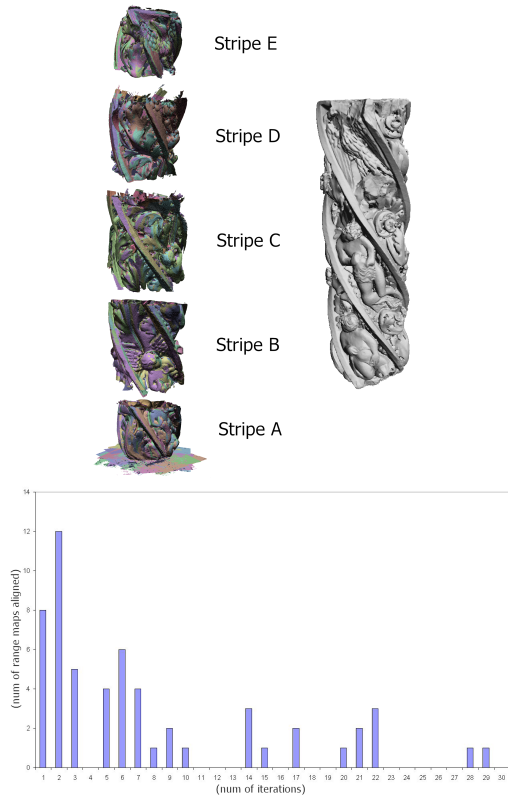


**Figure 6:** The result of the coarse alignment applied to the five circular stripes (left) and the final model obtained (bottom). The histogram shows how many range maps were aligned with that number of iterations; most of the alignments required less than 10 iterations.

Vivid 910, which returns range maps of resolution  $640 \times 480$  (around 300K samples). After the automatic selection of an initial coarse registration matrix with the proposed algorithm, all datasets were finely aligned (pairwise local registration, adjacency graph completion, and global registration) using our *MeshAlign* tool [CCG\*03]. The proposed algorithm was implemented in C++ language and all performance figures have been measured on a Pentium IV 2.4GHz PC with 1GB RAM.

### 6.1. Single range map pairs alignment

Figure 4 shows a set of three matching points selected on two range maps sampling a portion of the emperor Arrigo VII's head (the results are shown over the depth maps, rendered with no roto-translations added at visualization time). In this case each range map contains about 150k vertices (here large portions in the 2D maps contain no data). The solution was found in 30.8 seconds, setting  $t = 20$  and  $coarse\_err = 1.0mm$ . The algorithm iterated four times to

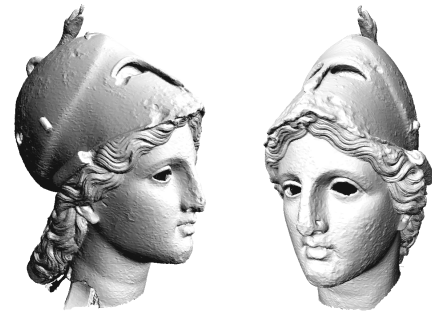


**Figure 7:** The minerva's head.

converge to a coarse alignment satisfying  $coarse\_err$ . The graph presents the best alignment error  $\epsilon_j$  obtained in the four iterations. The result of this coarse alignment is presented in the bottom part of Figure 4 (this figure must be seen in color since the two range maps are rendered with a different color). From this figure it is clear that the two range maps are sufficiently close for the ICP algorithm can be applied successfully to the meshes.

Another interesting example is shown in Figure 5; the matching points selected on two different range maps represent the back section of the Arrigo's head. In this case the running time was longer, 1 minute 28 seconds, since the algorithm was temporarily trapped in local minima and thus required more iterations than the previous example (9 in total, with 2 local minima). After the stall's detection (at the 5<sup>th</sup> iteration), the current solution was perturbed; we can notice that, at the next iteration, the solution found was worse than the previous one. Initially the error increases, but it improves in the subsequent iteration.

### 6.2. Stripes alignment

We now present some tests performed on large datasets. Figure 6 shows the result of the stripe-based alignment of a spiral column with artistic carvings (real size is about 85 cm tall, with a diameter of 25 cm.). Five circular stripes were scanned, for a total of 62 range maps (about 11M vertices). The automatic coarse alignment process completed in 1h:13min, using  $t = 20$  and  $coarse\_err = 1.0mm$ . The graph on the bottom of Figure 6 shows how many range maps of the column were aligned by the algorithm in a certain number of iterations: most of the range map pairs required few iterations ( $\leq 10$ ), while only 2 meshes required about thirty iterations. Another example of circular stripe is represented by the minerva's head (see Figure 7), the performances to align the dataset are shown in table 1. An example concerning a bas-relief is shown in Figure 8; the length of the bas-relief is approximately 2.5 meters. In this case two raster-scan (snake-like) stripes were acquired, for a total of 117 meshes (about 45.5M vertices). The algorithm performed the overall alignment in 1h:50min. As shown in the graph pre-



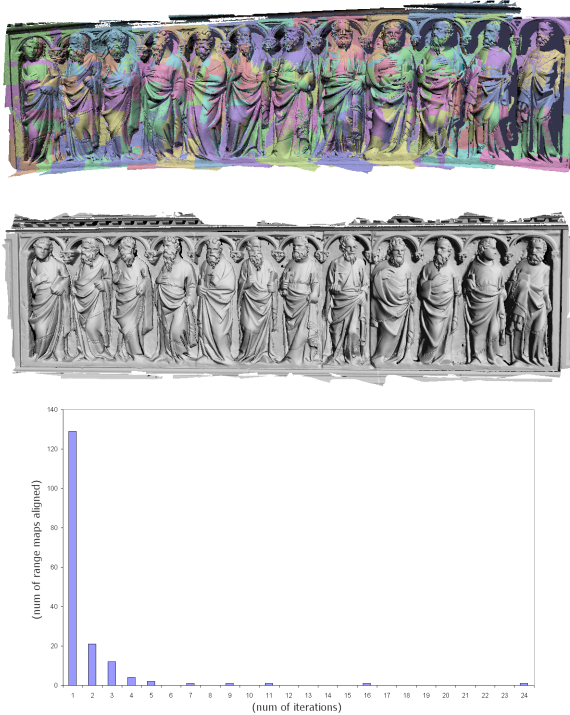


**Figure 8:** The coarse alignment of the bas-relief (top) and the final model (middle); almost all of the alignments required just 1 iteration.

sented in Figure 8, almost all the pair-wise alignments were done in a single iteration, so the entire process required a shorter time to complete than the previous example. This run produced an overall alignment completely satisfactory for the subsequent application of ICP and global alignment. Again, the set of arcs has been completed automatically by the *MeshAlign* system. It has to be underlined that all of the detected arcs are used by *MeshAlign* for the local and global fine registration step.

An overall presentation of numerical figures data of the processing of all the scans set is given in Table 1. The last two scan sets in this table are presented in Fig. 9 and 10.

## 7. Conclusions

We have presented an automatic registration method which has demonstrated very good performance while converging to valid solutions. The method is based on some simplifying assumptions, which allow us to solve the automatic registration with an iterative solution based on the automatic detection of corresponding point pairs and automatic detection of matching range maps pairs. The solution presented is based on a new shape characterization kernel that focuses on surface vertices; it works in the 2D space of the range



**Figure 9:** The coarse alignment of a portion of the archway of S. Ranieri's door, Pisa Cathedral (left). The final model after ICP and global alignment (right).

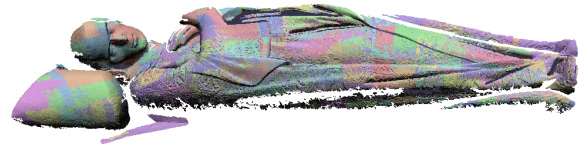


**Figure 10:** The coarse alignment of Arrigo VII's sepulcro.

maps and characterizes 3D geometry by processing surface normals evaluated on a kernel of regularly sampled adjacent points. The method has been shown to work well on real complex scan sets with good performance on standard PCs. We have included this solution as a background process in our scanning front end (which drives a Konica Minolta scanner). Due to the low computational complexity, automatic alignment runs in background during the acquisition, permitting on the fly alignment of the range maps. This allows the user to monitor the completion status of the acquisition and to detect not sampled surface regions well in advance, while removing the registration bottleneck.

## References

- [BAGC05] BRUSCO N., ANDRETTA M., GIORGI A., CORTELAZZO G.: 3D registration by textured spin-images. In *3DIM'05: Fifth Int. Conf. on 3D Digital Imaging and Modelling* (June 13-16 2005), IEEE Comp. Soc., p. (in press).
- [BDW\*04] BENDELS G. H., DEGENER P., WAHL R., KÖRTGEN M., KLEIN R.: Image-based registration of 3d-range data using feature surface elements. In *5th International Symposium on Virtual Reality, Archaeology and Cultural Heritage (VAST 2004)* (December 2004), Chrysanthou Y., Cain K., Silberman N., Niccolucci F. (Eds.), Eurographics, pp. 115–124.
- [BM92] BESL P. J., MCKAY N. D.: A method for registration of 3-D shapes. *IEEE Transactions on Pattern Analysis and machine Intelligence* 14, 2 (Feb. 1992), 239–258.
- [CCG\*03] CALLIERI M., CIGNONI P., GANOVELLI F., MONTANI C., PINGI P., SCOPIGNO R.: VCLab's tools for 3D range data processing. In *VAST 2003* (Bighton, UK, Nov. 5-7 2003), Eurographics, pp. 13–22.

Dataset	Range maps	Total vertices	Alignment time	No. pair-wise arcs (after adjac. augmentation)
Minerva's head	10	1.7M	7min	17
Spyral column (Arrigo VII)	62	11M	1h 13min	332
Bass-relief (Arrigo VII)	163	45.5M	1h 50min	1635
Bass-relief (Archway)	110	30M	52min	521
Sepolcro (Arrigo VII)	136	28M	41min	1944

**Table 1:** Numerical figures on the dataset considered in the empirical experiments.

- [CF01] CAMPBELL R. J., FLYNN P. J.: A Survey Of Free-Form Object Representation and Recognition Techniques. *Computer Vision and Image Understanding* 81, 2 (2001), 166–210.
- [CFI\*04] CALLIERI M., FASANO A., IMPOCO G., CIGNONI P., SCOPIGNO R., PARRINI G., BIAGINI G.: Roboscan: An automatic system for accurate and unattended 3d scanning. In *3DPVT'04: Tessaloniki, Greece* (Sept. 6-9 2004), IEEE Comp. Soc., pp. 805-812.
- [CHC99] CHEN C.-S., HUNG Y.-P., CHENG J.-B.: Ransac-based darces: A new approach to fast automatic registration of partially overlapping range images. *IEEE Transactions on Pattern Analysis and Machine Intelligence PAMI-21*, 11 (1999), 1229–1234.
- [CJ97] CHUA C. S., JARVIS R.: Point signatures: A new representation for 3d object recognition. *Int. J. Comput. Vision* 25 (1997), 63–85.
- [CM92] CHEN Y., MEDIONI G.: Object modelling by registration of multiple range images. *International Journal of Image and Vision Computing* 10, 3 (1992), 145–155.
- [DHI92] DELINGETTE H., HEBERT M., IKEUCHI K.: Shape representation and image segmentation using deformable surfaces. *Image and vision computing* 10 (1992), 132–144.
- [DHI93] DELINGETTE H., HEBERT M., , IKEUCHI K.: A spherical representation for the recognition of curved objects. In *Proc. IEEE Int. Conf. On Computer Vision* (1993), pp. 103–112.
- [FB81] FISCHLER M., BOLLES R.: Random sample consensus: A paradigm for model fitting with application to image analysis and automated cartography. *Communications of the ACM* 24, 6 (June 1981), 381–395.
- [HH03] HUBER D., HEBERT M.: Fully automatic registration of multiple 3d data sets. *Image and Vision Computing* 21, 7 (July 2003), 637–650.
- [JH97] JOHNSON A., HEBERT M.: Surface registration by matching oriented points. In *3DIM97* (1997), pp. 121-129.
- [LLC02] LUCA LUCCHESI G. D., CORTELAZZO G. M.: A frequency domain technique for range data registration. *IEEE Trans. on Pattern Analysis and Machine Intelligence* 24, 11 (2002), 1468–1484.
- [LPC\*00] LEVOY M., PULLI K., CURLESS B., RUSINKIEWICZ S., KOLLER D., PEREIRA L., GINZTON M., ANDERSON S., DAVIS J., GINSBERG J., SHADE J., FULK D.: The Digital Michelangelo Project: 3D scanning of large statues. In *SIGGRAPH 2000, Computer Graphics Proceedings* (July 24-28 2000), Annual Conference Series, Addison Wesley, pp. 131–144.
- [LR01] LEVOY M., RUSINKIEWICZ S.: Efficient variants of the ICP algorithm. In *Third Int. Conf. on 3D Digital Imaging and Modeling (3DIM 2001)* (May 28th - June 1st 2001), IEEE Comp. Soc., pp. 145–152.
- [MKR03] M. KAZHDAN T. F., RUSINKIEWICZ S.: Rotation invariant spherical harmonic representation of 3d shape descriptors. In *Eurographics Symposium on Geometry Processing* (2003), pp. 156–164.
- [MKR04] M. KAZHDAN T. F., RUSINKIEWICZ S.: Shape matching and anisotropy. *ACM Trans. on Graphics (SIGGRAPH 2004)* 23, 3 (Aug. 2004), pp. 623 - 629.
- [Pol03] POLHEMUS: The FastSCAN Cobra scanning system. <http://www.polhemus.com>, 2003.
- [Pu199] PULLI K.: Multiview registration for large datasets. In *Proc 2nd Int.l Conf. on 3D Digital Imaging and Modeling* (1999), IEEE, pp. 160–168.
- [Rot99] ROTH G.: Registering two overlapping range images. In *3DIM'99: Second Int. Conf. on 3D Digital Imaging and Modelling* (October 1999), pp. 191–200.
- [SM92] STEIN F., MEDIONI G.: Structural indexing: Efficient 3-d object recognition. *IEEE Trans. Pattern Anal. Mach. Intell.* 14 (1992), 125–145.
- [SPK\*03] SUN Y., PAIK J., KOSCHAN A., PAGE D., ABIDI M.: Point fingerprint: A new 3-d object representation scheme. *IEEE Transactions on Systems, Man and Cybernetics* 33, 4 (Aug. 2003), 712–717.
- [Ste04] STEINBICHLER OPTOTECHNIK: COMET series. <http://www.steinbichler.de>, 2004.
- [VS01] VRANIC D., SAUPE D.: 3D model retrieval with spherical harmonics and moments. In *Proc. of the DAGM* (2001), pp. 392–397.
- [WG02] WYNGAERD J. V., GOOL L. V.: Automatic crude patch registration: Toward automatic 3d model building. *Computer Vision and Image Understanding* 86, 2 (2002), 8–26.